SDC-91-00085

SDC
SOLENOIDAL DETECTOR NOTES

BEAM TEST ON RADIATION HARDNESS OF A SCINTILLATING TILE/FIBER CALORIMETER

October 15,1991

S. Funaki, K. Hara, T. Iinuma, T. Kaneko, S. Kim, K. Kondo,
Y. Miyamoto, S. Miyashita, Y. Morita, I. Nakano, M. Okabe, J. Suzuki,
H. Takahashi, K. Takikawa, N. Uemura and K. Yasuoka
Institute of Physics, University of Tsukuba

F. Abe, A. Asami, A. Enomoto, K. Furukawa, N. Kamikubota,
T. Kamitani, H. Kobayashi, M. Mishina, S. Ohsawa and Y. Yoshimura
National laboratory for High0Energy Physics (KEK)

SDC 91–00085
UTPP–39
October 15, 1991

Beam Test on Radiation Hardness of a Scintillating Tile/Fiber Calorimeter

S. Funaki, K. Hara, T. Iinuma, T. Kaneko, S. Kim, K. Kondo,Y. Miyamoto, S. Miyashita, Y. Morita, I. Nakano, M. Okabe, J. Suzuki, H. Takahashi, K. Takikawa, N. Uemura, and K. Yasuoka

Institute of Physics, University of Tsukuba, Tsukuba-shi, Ibaraki-ken 305, Japan

F. Abe, A. Asami, A. Enomoto, K. Furukawa, N. Kamikubota, T. Kamitani, H. Kobayashi, M. Mishina, S. Ohsawa, and Y. Yoshimura

National Laboratory for High-Energy Physics (KEK), Tsukuba-shi, Ibaraki-ken 305, Japan

(to be submitted to Nucl. Instrum. and Methods A)

Abstract

Radiation hardness of scintillating tile/fiber calorimeters is studied by irradiating electromagnetic test modules by 2.5-GeV electrons at the KEK linac. The induced damage is evaluated in a 2-GeV electron test beam by measuring a reduction of the pulse heights before and after irradiation. The pulse height peak for 2-GeV electrons is found to decrease by 19.3 $\pm$ 1.3% for a dose of 0.61 Mrad and 14.9 $\pm$ 2.7% for 0.33 Mrad. In addition to these modules, numbers of tile/fiber assemblies were irradiated up to 4.8 Mrad and the damage as a function of dose was measured with a radioactive source. Effects of radiation damage on the linearity and the energy resolution at higher energies are evaluated using a GEANT simulation code and the measured damage.

1 Introduction

Scintillating tile calorimeters with waveshifting fiber readout (tile/fiber calorimeters) are being developed as a candidate for precision calorimetry in the SSC experiment [1]. Radiation hardness is an important issue for calorimeters running in the high radiation environment in SSC detectors. The maximum radiation dose that occurs at electromagnetic shower maximum is estimated [2] to be 58 krad at pseudorapidity $\eta = 1.5$ and 5.7 Mrad at $\eta = 3$ for 10 years of operation at a design luminosity of 10^{33} cm^{-2}sec^{-1}. The average transverse momentum of minimum-bias π^0's that contribute mainly to the dose deposition is 0.6 GeV/c at the SSC energy.

Several groups have reported on radiation damage to scintillating tiles or fibers induced by radioactive sources or low-energy electron beam of several MeV[3]. Recently we have performed a series of measurements using a ^{60}Co source, which is described elsewhere[4]. In this paper, we report radiation hardness tests of real electromagnetic test modules using 2.5-GeV electron beam at the KEK linac. The energy deposition in the test module induced by 2.5-GeV electron shower is similar to that expected in the SSC experiment. The goal of this experiment is to investigate systematic effects of radiation damage on the performance as a calorimeter.

We constructed four test modules (Modules A to D) consisting of 21 layers of scintillating tiles and lead absorber plates. Modules A to C were irradiated to 0.61 Mrad, 0.33 Mrad and 4.8 Mrad, respectively, and Module D was kept from irradiation as a reference. The calorimeter response of Modules A and B was measured before and after irradiation in a 2-GeV electron test beam at the KEK 12-GeV proton synchrotron. In addition to these complete modules, numbers of scintillating tile/fiber assemblies were irradiated by placing the assemblies between the lead absorber plates. A set of 11 tile/fiber assemblies were irradiated at a time and were replaced with the new one at a dose of 0.31 Mrad, 0.96 Mrad and 1.2 Mrad: They are respectively named "Modules" E_1, E_2 and E_3. Radiation damage to the individual tiles of Modules C and E_1 to E_3 was measured as a function of dose by scanning with a ^{106}Ru source.

In Sec. 2 we describe the construction of the test modules, experimental procedures of irradiation by 2.5-GeV electrons and a measurement of the dose. Test beam measurements of the calorimeter performance are described in Sec. 3. In Sec. 4 we describe the ^{106}Ru source measurement of the damage as a function of dose. Section 5 is devoted to a Monte Carlo study on the radiation-induced degradation of the calorimeter performance. We summarize the results in Sec. 6.

2 Irradiation of Tile/Fiber Modules

2.1 Tile/fiber test modules

Figure 1 shows a schematic view of the tile/fiber test module. The module consists of 21 layers of 6.35 mm thick lead and 3 mm thick scintillating tile. The cross sections of the tile and the lead plate are 11.1 cm square and 13.5 cm square, respectively. The scintillating tile was Kuraray SCSN-81. A U-shaped groove 1.1 mm deep and 1.1 mm wide was machined

on the tile as shown in the figure. A waveshifting fiber 1 mm in diameter was embedded in the machined, non-polished groove to carry the scintillation light to photomultiplier tubes (PMTs) at the rear. We used Y-7 waveshifting fiber manufactured by Kuraray. The concentration of Y-7 was 150 ppm. The edges of the tile were polished and then the tile was wrapped with white paper for better light reflection. At 10 cm from the tiles the waveshifting fibers were spliced to Kuraray clear optical fibers that coupled to PMTs (Hamamatsu R580) through a light mixer. Both ends of a fiber were viewed by two different PMTs. The acrylic light mixer was optimized to a box shape of 3 cm $\times$ 3 cm in cross section and 7.5 cm in length. The gain of the PMTs was monitored by measuring the current output of the last 21st layer of scintillator, to which a ^{106}Ru source was attached. The radiation damage to this reference tile is expected to be negligible.

The dose given to the test module was measured with dosimeters stuck on the tiles. We used two types of dosimeter, Radiachromic Dye (RCD) film [5] and Cellulose Triacetate (CTA) film [6]. The difference in transmission at specific wavelengths before and after irradiation is a function of the absorbed dose[7]. In order to measure the longitudinal distribution of doses, two pieces of 1 cm $\times$ 1 cm RCD film were placed at the center of each tile except for the fourth one. On the fourth layer, at the shower maximum, 61 pieces of 1 cm $\times$ 1 cm RCD film and a CTA film with a cross section of 11 cm $\times$ 11 cm were stuck covering the entire surface to measure the lateral uniformity of the dose.

We constructed four complete modules. Prior to assembly, we measured the light yield of each tile/fiber assembly by injecting UV light at the center of the tile. The measured light yields were different by as much as 11%. We therefore selected the tile/fiber assemblies that have a similar light yield within a peak-to-peak deviation of $\pm 2\%$ to form a module. In addition to these complete modules, numbers of tile/fiber assemblies were made and irradiated at specific depths of the lead absorber stack (Modules E_1 to E_3). In order to compare directly with the results obtained from ^{60}Co exposure, the waveshifting fibers of these assemblies were not spliced to clear fibers.

2.2 Irradiation by 2.5-GeV electrons

Figure 2 shows the experimental setup at the KEK linac used to irradiate the test modules by 2.5-GeV electrons. Three modules were set at a time on a horizontally movable stage, with which one of the modules was positioned on the beam line with an accuracy better than 1 mm. Lead blocks laid in front of the stage kept the other modules from being irradiated. With a pair of steering magnets placed about 15 m upstream we scanned the module surface with the electron beam. The power supplies for these steering magnets were computer controlled through a GPIB-CAMAC interface. Two quadrupole magnets, installed with an intention to control the beam size, were not used in the actual irradiation.

The beam intensity was measured with a wall-current monitor (WCM), which was attached to the beam pipe upstream of the quadrupole magnets. The induced charge was read out with a CAMAC ADC module, LeCroy 2249A. The pulse width of the electron beam measured with the WCM was about 2 ns at the base and the intensity was typically 2×10^9 electrons per pulse.

To measure the beam profile we used a segmented wire ionization chamber (SWIC) placed right in front of the stage. The SWIC has an effective area of 16 cm $\times$ 16 cm, consisting of

X and Y chamber planes each with 64 strips, and provides a beam profile projected in the vertical and horizontal directions. The induced current from each strip was read out with ADCs, LeCroy 2249W. Two fluorescent screens, one near the WCM and the other on the SWIC, were used to monitor beam positions by TV cameras.

The electron beam profile measured with the SWIC was roughly a Gaussian shape with an rms width of about 4–5 cm. In order to uniformly irradiate the module, we scanned an area of 13 cm $\times$ 13 cm about the module center by sweeping the beam at a step interval of 1 cm. The linac provided the electron pulses at a repetition rate from 1 to 6 Hz. To reduce the possible fluctuation of the measurement system and of the electron beam, the beam was swept quickly every 8 pluses, *i.e.* every 1.3 sec to 8 sec, and the module was scanned over the surface many times. Modules A, B and E_1 were irradiated by rotating in turn the scanning patterns of (a) to (d) shown in Fig. 3. For the other modules, we irradiated additionally the boundaries of the module according to pattern (e) to obtain a more uniform dose distribution.

Each module was irradiated for typically 1 to 2 hours per day until the dose reached the scheduled amount. The irradiation took place from May 23 to July 20, 1991.

2.3 Uniformity of the dose

The dose during the irradiation was evaluated using the measured beam intensity and the profile. The energy deposition in the tiles per unit beam intensity was calculated using a GEANT simulation code. After the irradiation was completed, we measured the absorbed dose using the RCD dosimeter. Figure 4 shows a lateral distribution of the dose measured at the fourth layer of Modules B and E_2. The dose at the tile edge is substantially smaller than that at the center. The average doses in 5 cm square around the center are 451 krad, 6.1 Mrad, 1.3 Mrad and 1.5 Mrad for Modules B, C, E_2, and E_3, respectively, while those at the edge (within 1 cm from the edge) are 236 krad, 4.2 Mrad, 0.77 Mrad and 1.0 Mrad. Since Module E_1 and Fermilab/Purdue modules F_1 and F_2 were not equipped with dosimeters covering the full surface and Module A is being kept from reassembled, we have to rely on these measurements of dose non-uniformity. Modules A, B and E_1 were irradiated in a similar way, so that, as the dose uniformity of these modules, we quote the measured value of 52% for Module B. The measured uniformity of Modules C, E_2 and E_3 was between 60% and 69%, and for Modules F_1 and F_2 irradiated in a similar way as the above three, we assumed the same value of dose uniformity.

Table I summarizes the irradiation conditions for Modules A to F. The dose at center, the dose at edge and the mean dose are listed in the table, together with the instantaneous and average dose rates. The instantaneous dose rate is a dose rate during the period the module was exposed to the electron beam. The average dose rate is the mean dose divided by the calendar days. The uncertainties in the dose measurement are about 10%. Also listed in the table is the method of measuring the damage. Modules F_1 and F_2 were sent back to Fermilab after irradiation.

Since the lateral dose distribution was not uniform, we evaluated the effect of non-uniform dose on the light yield. We exposed several tile/fiber assemblies to ^{60}Co, one group uniformly and another non-uniformly with edges shielded by iron plates. Before and after the irradiation the light yield of the tile/fiber excited by a ^{106}Ru source was measured as described in

Sec. 4. Figure 5 plots the induced damage, a ratio of currents before and after the irradiation, and a fitted curve as a function of the dose [4]. We irradiated three samples to 0.62 Mrad at the center, with a dose at the edge being decreased to 71%, 47% and 33% of the dose at center. As shown in the figure, these samples showed somewhat smaller damage than the uniformly irradiated sample. An effective dose for the non-uniformly irradiated sample could be evaluated as the dose at which the uniform sample shows the same amount of damage. The effective dose calculated in this way is consistent with the mean of the non-uniform dose to within 15%. In this paper, unless otherwise specified, we use the mean dose as the dose given to the tile/fiber assembly by the electron beam.

Figure 6 plots the dose measured at the tile center as a function of the layer number in the module. Plotted together is a simulated shower curve for 2.5-GeV electrons, normalized by the area. The shower profile measured by the dosimeter is reproduced well by the simulation.

3 Measurements with Electron Test Beam

3.1 Experimental apparatus

Modules A and B were calibrated before and after the irradiation in an electron test beam at π-2 beam line of the KEK 12-GeV proton synchrotron. Figure 7 shows the experimental setup at the test beam line. Energy response of the modules was measured in an electron beam with a momentum range from 0.5 to 3 GeV/c. Electrons were tagged by the Spot Trigger, $\mathtt{S0} \cdot \mathtt{S1} \cdot \mathtt{S2} \cdot \mathtt{S3} \cdot \mathtt{S4} \cdot \mathtt{GC} \cdot \overline{\mathtt{S5}}$, where S0 – S5 were beam counters and GC was a gas Cherenkov counter. The gas Cherenkov counter was used to discriminate hadron contamination in the beam. The counter S5 placed behind the calorimeter module helped in suppressing the background hadrons and muons. The background remaining in the electron beam was typically 10%. The beam size defined by the smallest beam counter S4 was 1 cm $\times$ 1 cm.

We mapped the calorimeter response with 2-GeV/c electrons. The counter S4 was taken out from the trigger and the beam size was approximately 3 cm $\times$ 3 cm. The test module was placed on a movable stage and positioned at steps of 4 cm horizontally and vertically to cover the whole calorimeter surface. The impact point of the beam was reconstructed from hit channels of multi-wire proportional chambers which had a wire spacing of 1 mm and covered an area of 96 mm $\times$ 96 mm.

The beam spill was 0.5 sec with a repetition rate of 4.5 sec. The trigger rate was typically 30–60 electrons per pulse with the Spot Trigger. The momentum spread calculated using a simulation code TURTLE was $\pm$1.5% peak to peak at 2 GeV/c.

PMT signals of the test module were amplified and digitized by the RABBIT system[8]. The ADC has a 16-bit dynamic range and a sensitivity of 11 fC/count. The RABBIT PM-amplifier card uses two sample-and-hold circuits, Before and After gates, to measure the charge from the PMT. The PM-amplifier card measures on an event-by-event basis the current as well: The current data were used to monitor a gain stability of the PMTs. The pedestals were measured concurrently with the data taking by injecting trigger signals from the computer.

3.2 Pulse height peaks before and after irradiation

Module A (B) was measured in the electron test beam 11 (5) days after the electron beam exposure was stopped. Figure 8 shows the pulse height spectra for 2-GeV electrons, measured before and after the irradiation. Signals from the two PMTs were summed after adjusting a relative PMT gain. A Gaussian function was fitted to the data in a region around the peak with a linear function fitted to the background. The peak values thus determined and the statistical and systematic uncertainties are summarized in Table II. The ADC pedestals measured during the data taking were stable within 10–40 ADC counts. The pedestal fluctuation was included in the statistical error.

As regards the systematic errors, we considered the following two uncertainties. First, the gain stability of the PMTs was monitored by measuring the current induced by a ^{106}Ru source attached to the reference tile at the 21st layer. The ratio of the currents before and after the irradiation was consistent with that expected from the decay of ^{106}Ru to within 1.7%. Deviations from the expectation from the finite lifetime were corrected as a PMT gain drift. Figure 9 shows a history of the ^{106}Ru-induced current for Module B, which showed a larger gain variation than Module A. The current sum of two PMTs was stable with an rms fluctuation of 0.95% and 1.2% before and after the irradiation. The rms fluctuation was 0.6% and 0.7% for Module A. The systematic uncertainty originating from the PMT gain instability is estimated as a quadrature sum of these rms values, including conservatively the correction values for the gain drift. Second, the uncertainty in the fitted peak coming from the fitting procedure was investigated. This was evaluated to be 20 counts by trying the fit with different background subtraction and also by changing the fit region. The overall systematic uncertainty was estimated by adding in quadrature the above two uncertainties.

The pulse height peak decreased by 19.3±1.3% for Module A and 14.9±2.7% for Module B, where the errors include the statistical and systematic errors. The energy resolution of 2-GeV electrons, defined as a sigma of the fitted Gaussian function, changed from 17.1±0.4% to 17.4±0.5% for Module A and from 14.1±0.5% to 15.9±0.6% for Module B: The energy resolution is barely degraded in the energy range of this measurement.

The pulse height peak and the energy resolution are plotted in Fig. 10 as a function of the electron energy. The data are measured after the irradiation. Although the energy range is limited, the response is linear between 0.5 GeV and 3 GeV. The energy resolutions are fitted well by a curve $const/\sqrt{E}$.

3.3 Uniformity mapping with 2-GeV electrons

The scintillating tile is known to be colored after irradiation, which may introduce a change of response map across the tile. The response map was measured before and after the irradiation in the 2-GeV electron test beam. Typically 450k events were accumulated for each measurement.

The data were divided into meshes of 5 mm × 5 mm and the pulse height peak was searched for in each mesh. We used a summed pulse height of the two PMTs as the response at each mesh point. The response gradually decreases near the calorimeter boundary due to shower leakage and the peak is not obtainable in the outermost mesh points. In this case the peak was replaced with the mean and the error with the rms of the distribution. Figure 11

shows the response map of Module A after the irradiation of 0.61 Mrad. The response shape is mainly characterized by shower leakage. The dip behind is due to the notch in the lead plate for readout fibers. The statistical uncertainties in each data point are typically 1% and better than 2%.

In order to compare the response shapes before and after the irradiation, the fitted peaks were normalized by the pulse height peaks at the module center. Typical maps across the tile are shown in Fig. 12. The responses before and after the irradiation are similar in shape, indicating that the light yield decreases by a certain amount but the shape of the response map does not change.

Module A was irradiated non-uniformly with the dose at the edge being 52% of the dose at the center. We have exposed several tile/fiber assemblies to ^{60}Co non-uniformly as mentioned in Sec. 2.3. As shown in Fig. 13, the response shape measured with a ^{106}Ru source did not change even for the sample with the edge irradiated to only 33% of the center dose of 0.62 Mrad. The present result of the similarity in the response shape obtained with electron beam is consistent with this ^{60}Co exposure result. The scintillating light travels everywhere in the tile and the local non-uniform damage is averaged out. Since the radiation dose at large η changes rapidly in the SSC experiments, the tiles at large η are subjected to non-uniform irradiation. The present results suggest that even the tiles irradiated non-uniformly will maintain their response uniformity unchanged.

4 ^{106}Ru Source Measurement of Damage vs Dose

The tile/fiber assemblies of Modules C, E_1 and E_2 were measured with a ^{106}Ru source before and after the irradiation. The measurements after the irradiation were made two weeks after the electron beam exposure was stopped.

Each tile/fiber assembly was placed in a light shielded box made of 1-mm thick aluminum, where a reference assembly was kept fixed to the box. The readout fibers of the assembly under measurement and of the reference tile were viewed by a PMT (Hamamatsu R580). In each measurement a ^{106}Ru source was moved across the two tiles one after the other. The PMT current at each position was read out with a picoammeter, Keithley 485, through a GPIB interface. By taking a ratio of the currents from the tile under measurement and the reference tile, the possible gain variation of the PMT was reduced. The gain variation associated with setting up a tile/fiber assembly in the measuring device was verified to be less than 3%. More details on the measurement system can be found elsewhere[4].

Figure 14 shows the reduction of light yield of individual tiles measured with the ^{106}Ru source scan. The abscissa is the mean dose of individual tiles, obtained by applying the correction for the non-uniform irradiation to the measured dose at the center of each tile. We denote the reduction of light yield by $1 - d$, where d is a relative light loss, called the damage. The dose dependence of the damage induced by 2.5-GeV electron shower, shown in Fig. 14, is fitted well by the expression:

$$1 - d = 0.824\exp(-0.232D) + 0.157\exp(-7.39D), \tag{1}$$

where dose D is in Mrad. The damage induced by 2.5-GeV electron shower agrees roughly with that induced by ^{60}Co [4]. An example of the ^{60}Co induced damage is shown in Fig. 5.

5 Monte Carlo Study of Performance Degradation

We simulated the effects of radiation damage on the calorimeter performance using a GEANT code for electron shower development. The electron shower for a given energy was developed through the test module with the low-energy cutoff for electrons and photons set to 1 MeV. The energy deposition in each tile was stored on an event-by-event basis. In simulating the effects of radiation damage, the energy deposition in each tile is reduced according to the damage. The dose distribution along the depth was given by the average longitudinal shower profile of 2.5-GeV electrons. A peak dose and hence a peak damage occurs at the fourth tile in the geometry of our test module. For a given value of peak damage, we derived the corresponding value of dose from the measured curve of damage vs dose, Eq. (1). Once the peak dose was determined, the doses of the other tiles were scaled according to the longitudinal dose distribution, and their damages were calculated using Eq. (1). The reduced energy depositions in the tiles were summed on an event-by-event basis and the sum was converted to the number of photoelectrons with a Poisson fluctuation included. As for the conversion factor from the energy to photoelectrons, we used a value of 1.8 photoelectrons/mip obtained in a test bench measurement.

We first calculated the pulse height and the energy resolution for 2-GeV electrons as a function of the peak damage. The results are shown in Fig. 15. The energy response decreases monotonically with the peak damage. The energy resolution, on the other hand, is degraded only slowly. The measured pulse height reduction and energy resolutions before and after the irradiation are also plotted in the figure for comparison. The horizontal bar associated with the data point represents a range of peak damage corresponding to the dose at center and the dose at edge. Although the energy resolution for Module A is slightly larger than that expected by the simulation, the measured values are reproduced fairly well by the simulation.

We extend the Monte Carlo study to higher energies. Figure 16 shows the reduction of the energy response as a function of the electron energy for peak damages of 10% to 50%. At a peak damage of 30% the response reduces to 78% at 5 GeV and to 81% at 100 GeV, producing a non-linearity of the order of 3% in this energy range. This non-linearity in the 5 to 100 GeV range, however, seems to be expressed by a simple smooth function of the energy, which can be used for correcting the non-linear response. Note that the present calculation is based on a damage profile in calorimeter layers induced by 2.5-GeV electrons, but in the real experiment, the damage is induced by particles with various momenta. We calculated similar curves for damage profiles induced by 1-GeV and 10-GeV electrons. Although the magnitude of the non-linearity depends on the assumed energy, ranging from 5% to 2% for these energies at a peak damage of 30%, the non-linearity remains a smooth function of the energy. For the SSC experiment a couple of *in situ* energy calibration procedures are proposed [1], such as using high energy electrons from W and Z decays. Since such electrons show a fairly wide spread in energy, the smooth non-linearity can be verified by dividing the electrons into several energy bins. Measuring the longitudinal damage profile by scanning with a radioactive source provides the necessary data to correct for the non-linearity.

The energy resolution for higher energies was studied as a function of the peak damage. Figure 17 shows the normalized resolution, *i.e.*, resolution times $\sqrt{E\,(\text{in GeV})}$, as a function of the energy E for various peak damages. The normalized resolution degrades with the peak

damage especially at higher energies. The error in the resolution induced by damage shows up at higher energies. The resolutions are plotted as a function of the peak damage in Fig. 18 for electron energies of 20, 50 and 100 GeV. We extract the damage-induced error $\sigma_{\rm damage}$ by $\sigma^2_{\rm damage} = \sigma^2_{\rm meas} - \sigma^2_{\rm ND}$, where $\sigma_{\rm meas}$ is the measured resolution and $\sigma_{\rm ND}$ is the resolution at no damage. The obtained $\sigma_{\rm damage}$ is plotted in Fig. 19 for the same electron energies. The damage-induced error for 100 GeV electrons reaches 1% (2%) at a peak damage of 25% (39%). Similar results were obtained in Ref. [9], where the damage profile was assumed to be proportional to the energy depositions induced by 1-GeV or 10-GeV electrons. We also did similar calculations for 1-GeV and 10-GeV electrons using the measured relationship of damage vs dose. The results were essentially the same: The damage-induced error is insensitive to the detailed shape of the damage profile in the tiles, but is determined by the magnitude of the peak damage.

According to Eq. (1), the doses corresponding to peak damages of 25% and 39% are 0.44 Mrad and 1.3 Mrad, respectively.

6 Conclusions

We have constructed tile/fiber calorimeter modules using Kuraray SCSN-81 scintillating tile and Y-7 waveshifting fiber spliced to clear fiber, and irradiated by 2.5-GeV electrons up to a dose of 0.42 to 6.1 Mrad at the center of the shower maximum tile. The dose at the edge was between 52% and 69% of the dose at the center.

The induced damage of two modules irradiated to mean doses of 0.61 Mrad and 0.33 Mrad was measured in an electron test beam. The pulse height for 2-GeV electrons decreased by 19.3% and 14.9%, respectively. In an electron energy range from 0.5 to 3 GeV, the response after the irradiation was linear and the energy resolution was barely degraded.

The response to 2-GeV electrons was mapped over the calorimeter surface. The shape of the response map did not change for the module irradiated to 0.61 Mrad.

In addition to the electron test beam measurement, the radiation damage of individual tile/fiber assemblies was measured with a ^{106}Ru source in the dose range from 4 krad to 4.8 Mrad. The reduction of the light yield d is expressed as a function of dose D (in Mrad) by $1 - d = 0.824\ \exp(-0.232\ D) + 0.157\ \exp(-7.39\ D)$.

Degradation of the calorimeter performance was evaluated using a GEANT simulation and the measured damage curve. The simulation for 2-GeV electrons reproduces the pulse height reduction and energy resolution observed in this experiment. For a peak damage of 30%, the non-linearity of the response in an energy range from 5 to 100 GeV was found to be 2–5% depending on the assumed incident energy 1 GeV or 10 GeV of electrons that cause the radiation damage. This non-linearity is a smooth function of the energy and can be corrected for by using the *in situ* source calibration and the electrons from W and Z decays. For 100-GeV electrons the damage-induced error to resolution was found to increase to 1% at a peak damage of 25% and to 2% at a peak damage of 39%. The doses corresponding to these peak damages are 0.44 Mrad and 1.3 Mrad, respectively.

The tile/fiber calorimeter using SCSN-81 scintillator and Y-7 waveshifting fiber is a candidate for precision calorimetry in the barrel region $|\eta| \leq 1.5$ of the SDC detector. For the endcap $1.5 \leq |\eta| \leq 3.0$ we need to develop new plastics which is harder to radiation.

Acknowledgements

We would like to thank M. Sunaga of Japan Atomic Energy Research Institute (Takasaki), who performed the calibration of the dosimeters. K. H. Tanaka of KEK is also acknowledged, who has kindly provided us with the SWIC and its readout electronics. The experiment would not have been possible without the support of S. Ban and the KEK radiation safety staff, the KEK 2.5-GeV linac operation crews and the KEK proton synchrotron staff. Many thanks are due to G. W. Foster, D. R. Green and J. Proudfoot for helpful discussions, and G. H. Trilling and M. G. D. Gilchriese for their encouragement. The basic design of the present test module was provided by G. W. Foster. Finally we would like to express our appreciation to KEK Director General H. Sugawara and PS Experiment Coordinator K. Takamatsu for their encouragement throughout the experiment.

References

[1] G. H. Trilling *et al.*, "Solenoidal Detector Collaboration Expression of Interest," Solenoidal Detector Collaboration Note SDC-90-00085 (1990);
G. H. Trilling *et al.*, "Solenoidal Detector Collaboration Letter of Intent," Solenoidal Detector Collaboration Note SDC-90-000151 (1990).

[2] D. E. Groom, "Proc. of the 1988 Summer Study on High Energy Physics in the 1990's", ed. by F. J. Gilman and S. Jensen, Snowmass CO., July 1988 (1989);
"Report for the Task Force on Radiation Levels in the SSC Interaction Regions," ed. by D. E. Groom, SSC Central Design Group Report SSC-SR-1033 (June 1988).

[3] P. Bonamy *et al.* "Radiation Damage in Scintillating Plates and Fibers", Solenoidal Detector Collaboration Note SDC-91-00011 (1991);
For a recent review, see, for example, "Proceedings of the Workshop on Radiation Hardness of Plastic Scintillator", ed. by K. F. Johnson (1990), and references therein.

[4] S. Funaki *et al.*, paper in preparation.

[5] Far West Technologies, Goleta, CA., USA.

[6] Type FTR-125, Fuji photo film Co. Ltd., Tokyo 106, Japan.

[7] The dosimeters RCD and CTA films were calibrated with 2-MeV electron beam at Japan Atomic Energy Research Institute (Takasaki). The usable dose range of RCD films is 30 krad to 10 Mrad and of CTA films is 0.5 Mrad to 30 Mrad.

[8] G. Drake *et al.*, "CDF Front End Electronics: The RABBIT System", Nucl. Instrum. Methods A269 (1988) 68.

[9] D. Green, A. Para and J. Hauptman, "Radiation Damage, Calibration and Depth Segmentation in Calorimeters", Fermilab Note 565;
J. Hauptman, "EM Constant Term due to Radiation Damage in Scintillator", SDC Note Addenda, 1 July (1991).

Table I. Irradiation conditions for Modules A to F. The dose and dose rate refer to those at the shower maximum, the fourth layer, of the test module. The dose D_{cntr} is the average dose in 5 cm square around the center, D_{edge} is the average dose within 1 cm from the edges, and D_{mean} is the mean over the tile surface. The instantaneous dose rate DR_{inst} and the average dose rate DR_{av} are calculated using the mean dose. The uncertainty in the dose measured using dosimeters is about 10%. The numbers with a star are evaluated values using the dosimeter data of a module irradiated in similar conditions and the measured beam intensity. Irradiation of a module took place for typically 1–2 hours a day. The number of calendar days elapsed during the irradiation is shown in the column Time. Irradiation was done mostly in air, except that Modules E_3 and F_2 were irradiated in nitrogen gas.

Module	D_{cntr} (Mrad)	D_{edge} (Mrad)	D_{mean} (Mrad)	DR_{inst} (krad/h)	DR_{av} (krad/h)	Time (days)	air/N_2	Measured with
A	0.84*	0.44*	0.61*	110*	8*	3	air	e-beam
B	0.45	0.24	0.33	16	2	8	air	e-beam
C	6.1	4.2	4.8	140	8	24	air	Ru
D								Reference
E_1	0.42*	0.22*	0.31*	38*	3*	5	air	Ru
E_2	1.3	0.77	0.96	49	3	14	air	Ru
E_3	1.5	1.0	1.2	46	10	5	N_2	Ru
F_1	1.4*	0.88*	1.1*	53*	3*	14	air	sent to FNAL
F_2	1.5*	1.0*	1.2*	48*	10*	5	N_2	sent to FNAL

Table II. Pulse height peaks (ADC counts) for Modules A and B measured before and after irradiation. Systematic errors originating from the PMT gain drift are listed in parentheses.

Module	Before	After	Ratio	stat.	syst.	(PMT gain drift)
Module A	6060±31	4890±21	80.7%	±0.7%	±1.1%	(−0.6%)
Module B	6649±28	5657±24	85.1%	±0.6%	±2.7%	(−1.7%)

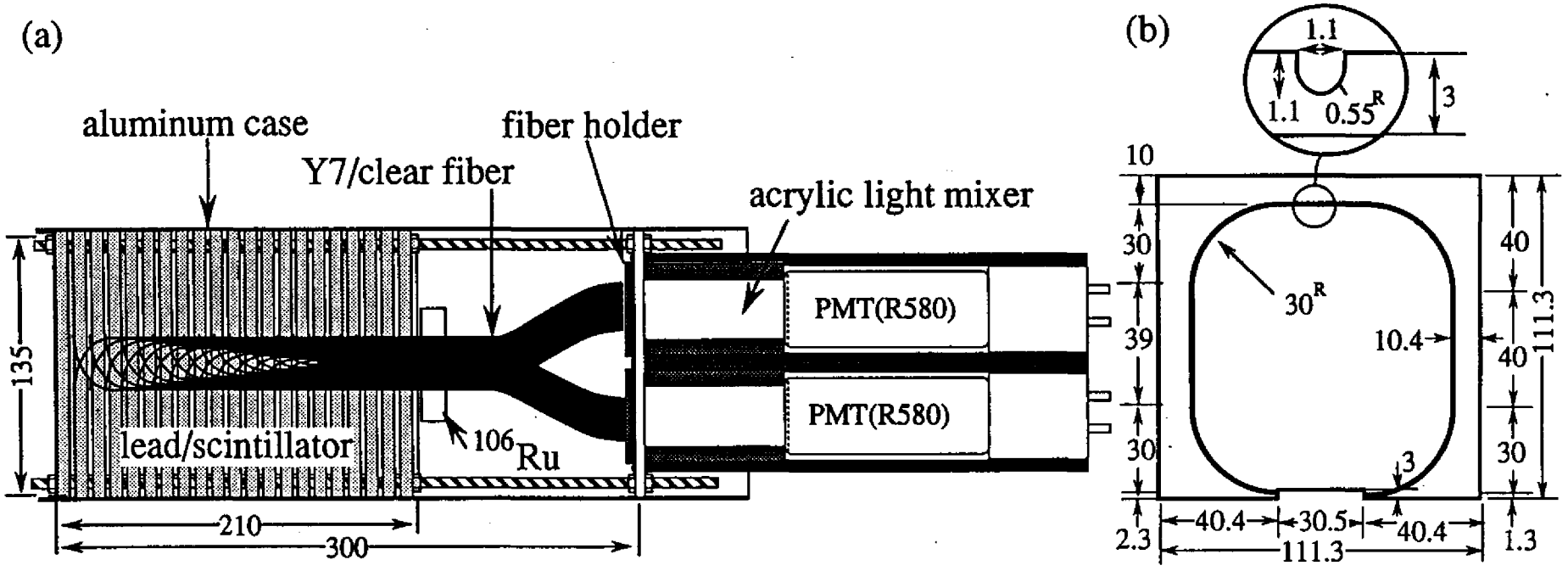

Figure 1: Schematic view of (a) the tile/fiber test module and (b) the scintillating tile with a groove for the readout fiber.

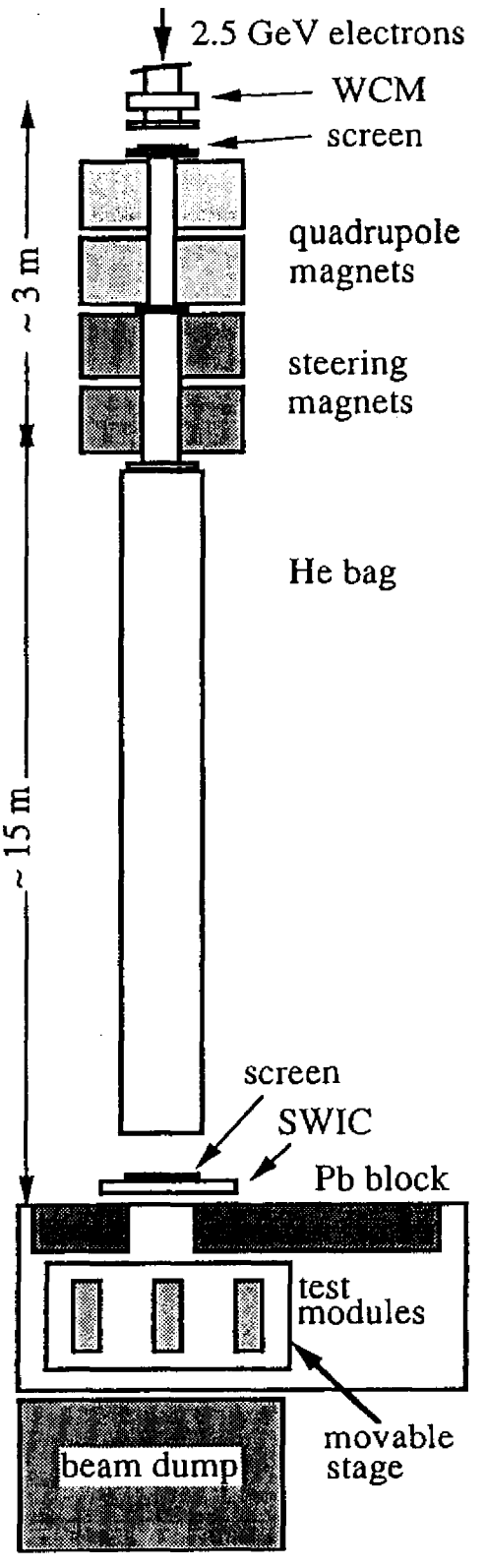

Figure 2: Experimental setup used for exposing 2.5-GeV electrons at the KEK linac.

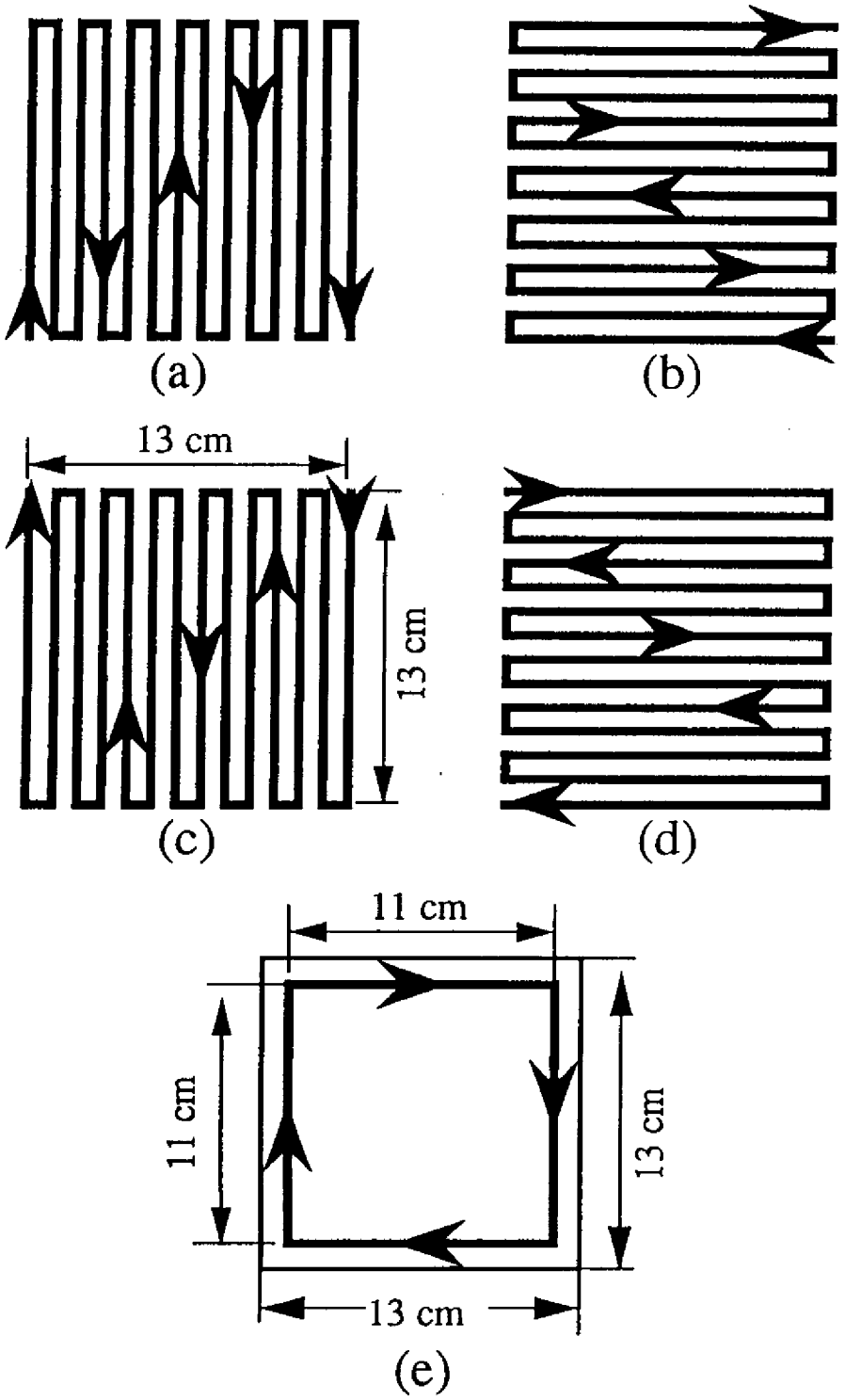

Figure 3: The beam was swept with a step of 1 cm by rotating in turn the scanning patterns (a) to (d). For some modules the tile boundaries were scanned additionally according to pattern (e).

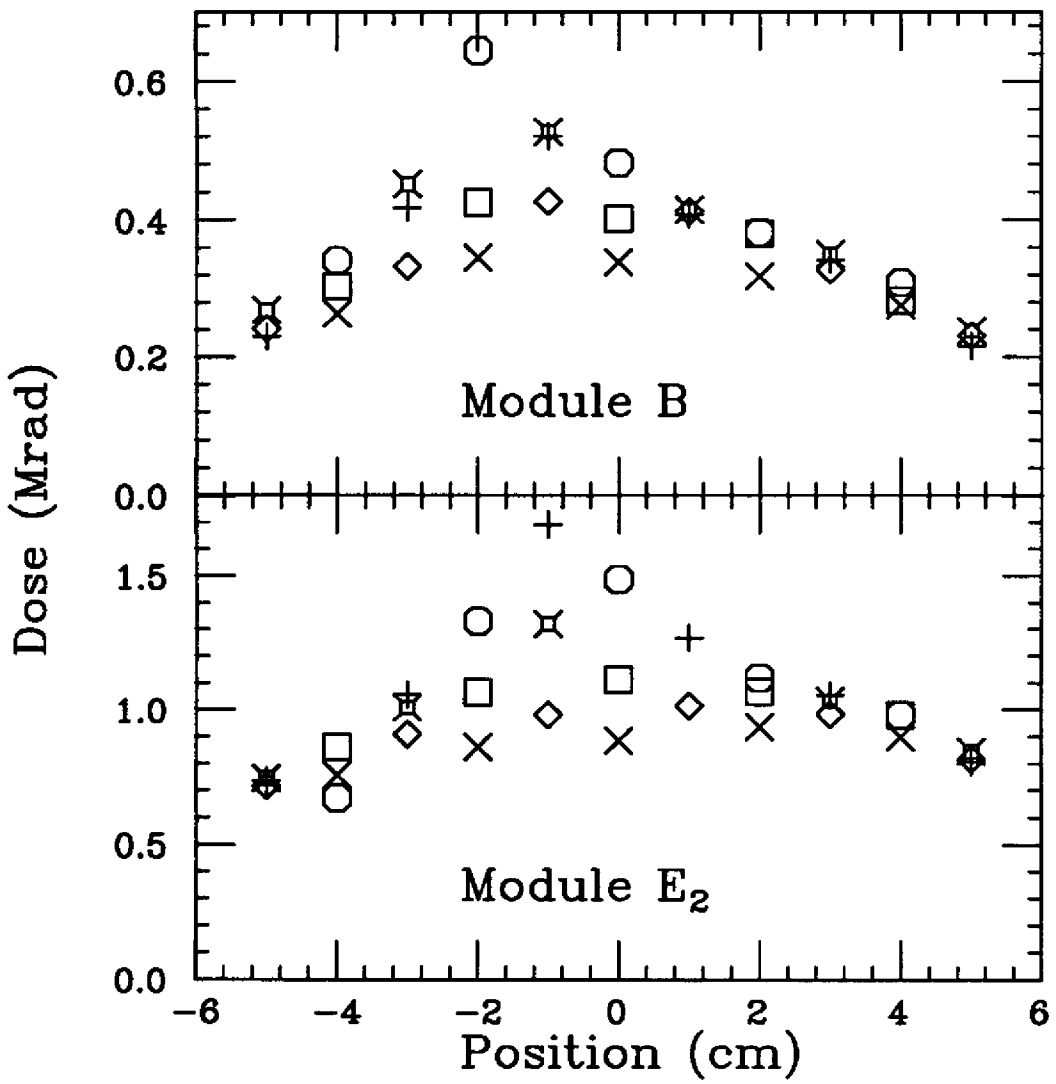

Figure 4: Dose measured using RCD dosimeter films as a function of the horizontal position. The data are shown for Modules B and E_2 with various marks indicating the vertical positions from the edge: 0.5 cm (cross), 1.5 cm (diamond), 2.5 cm (square), 3.5 cm (square-cross), 4.5 cm (circle) and 5.5 cm (plus).

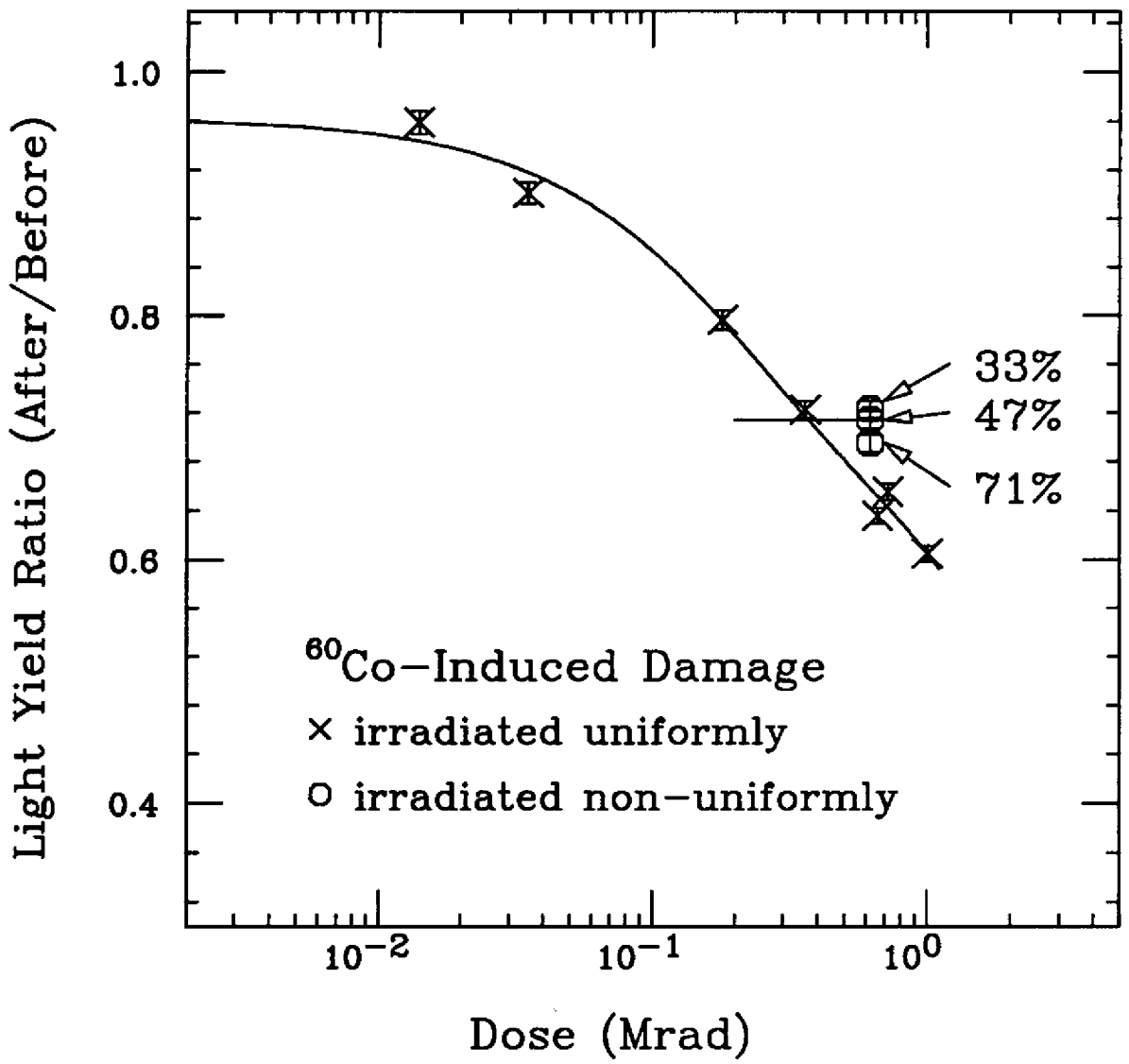

Figure 5: Measured light yield ratios for samples exposed to ^{60}Co uniformly and non-uniformly. Non-uniformly irradiated samples (circles) show smaller damage than the uniformly irradiated samples (crosses). The percentages quoted are the ratio of the doses at the edge and at the center for the non-uniformly irradiated samples.

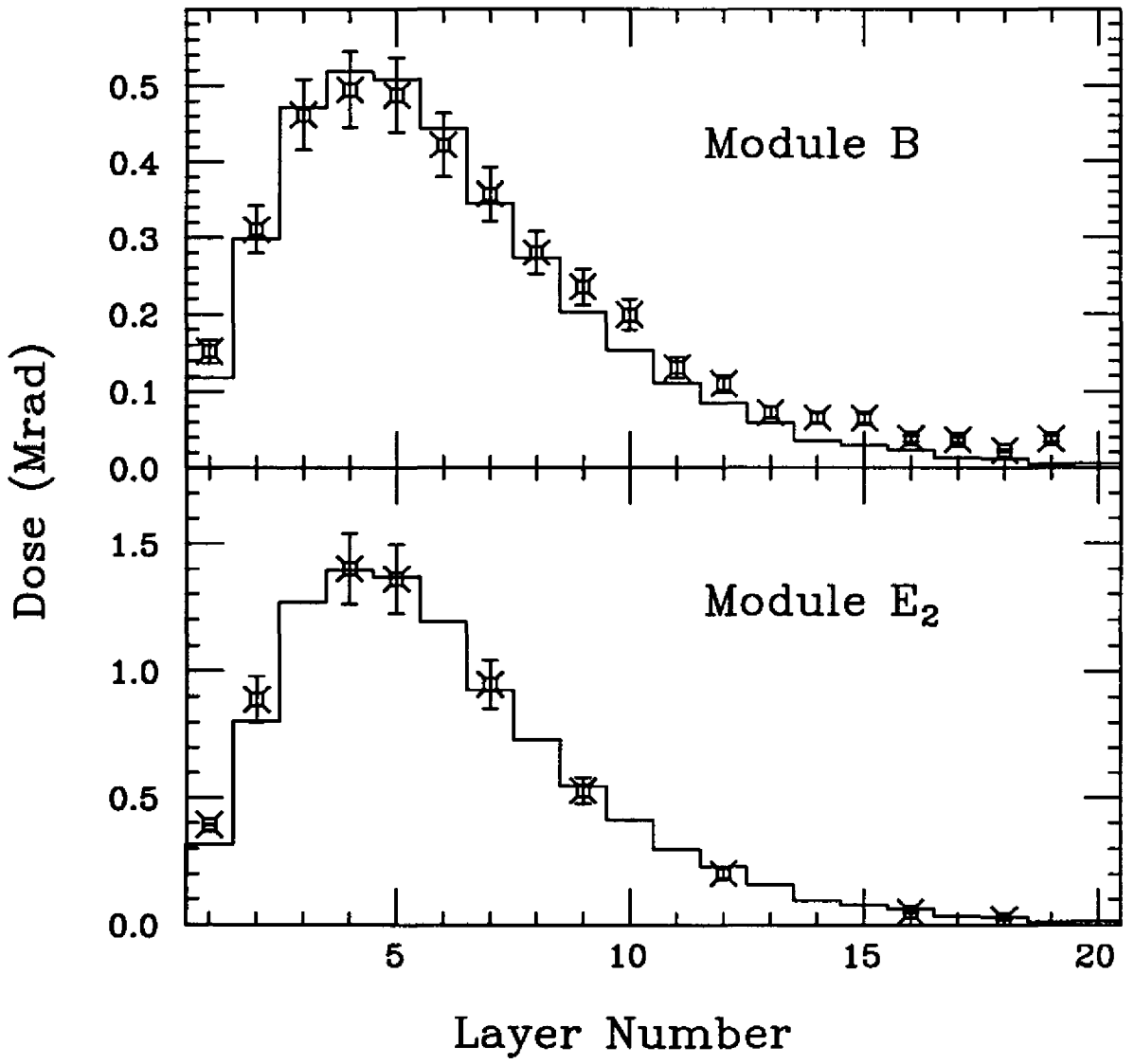

Figure 6: Dose as a function of the depth, measured using the RCD dosimeter films for Modules B and E_2. Data are compared with a shower curve calculated using a GEANT simulation code.

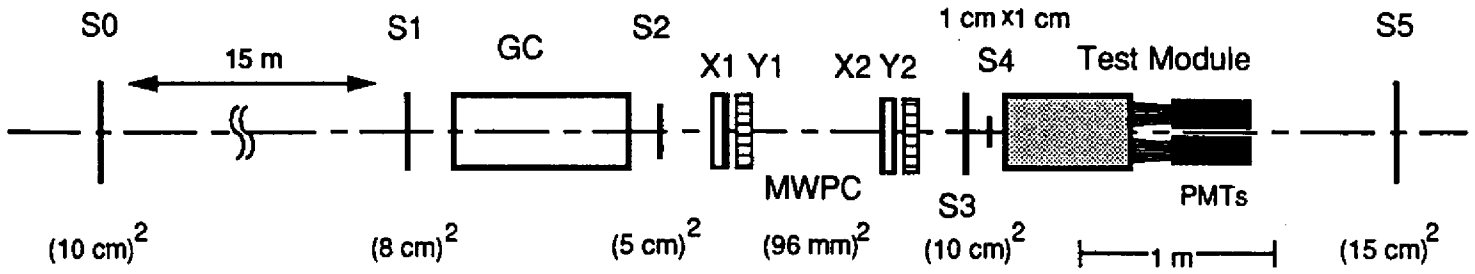

Figure 7: Experimental setup at the KEK proton synchrotron π-2 beam line.

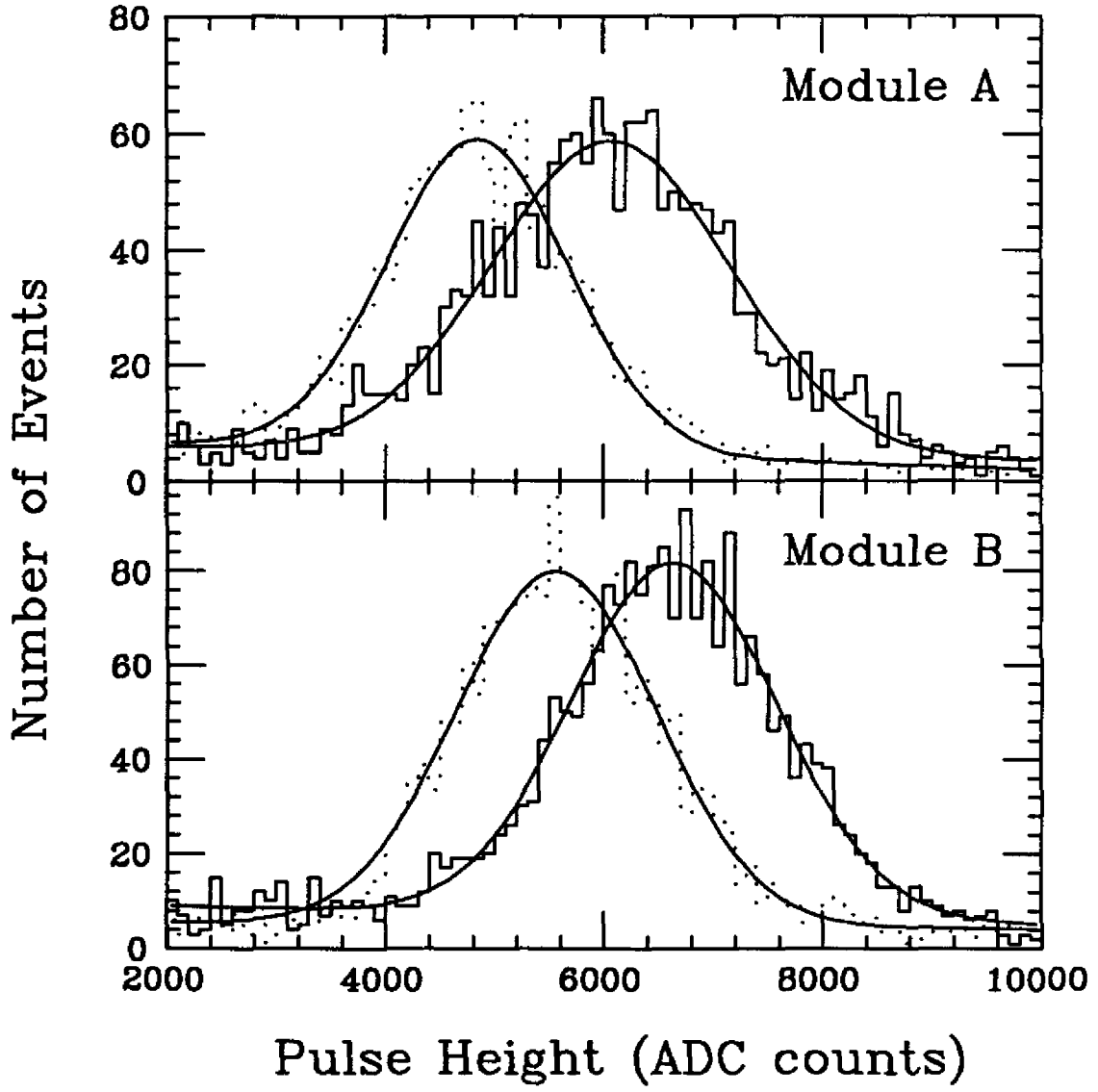

Figure 8: Pulse height distributions for Modules A and B measured with 2-GeV electrons. The pedestals are subtracted. The distributions before (solid histogram) and after (dotted histogram) irradiation are compared.

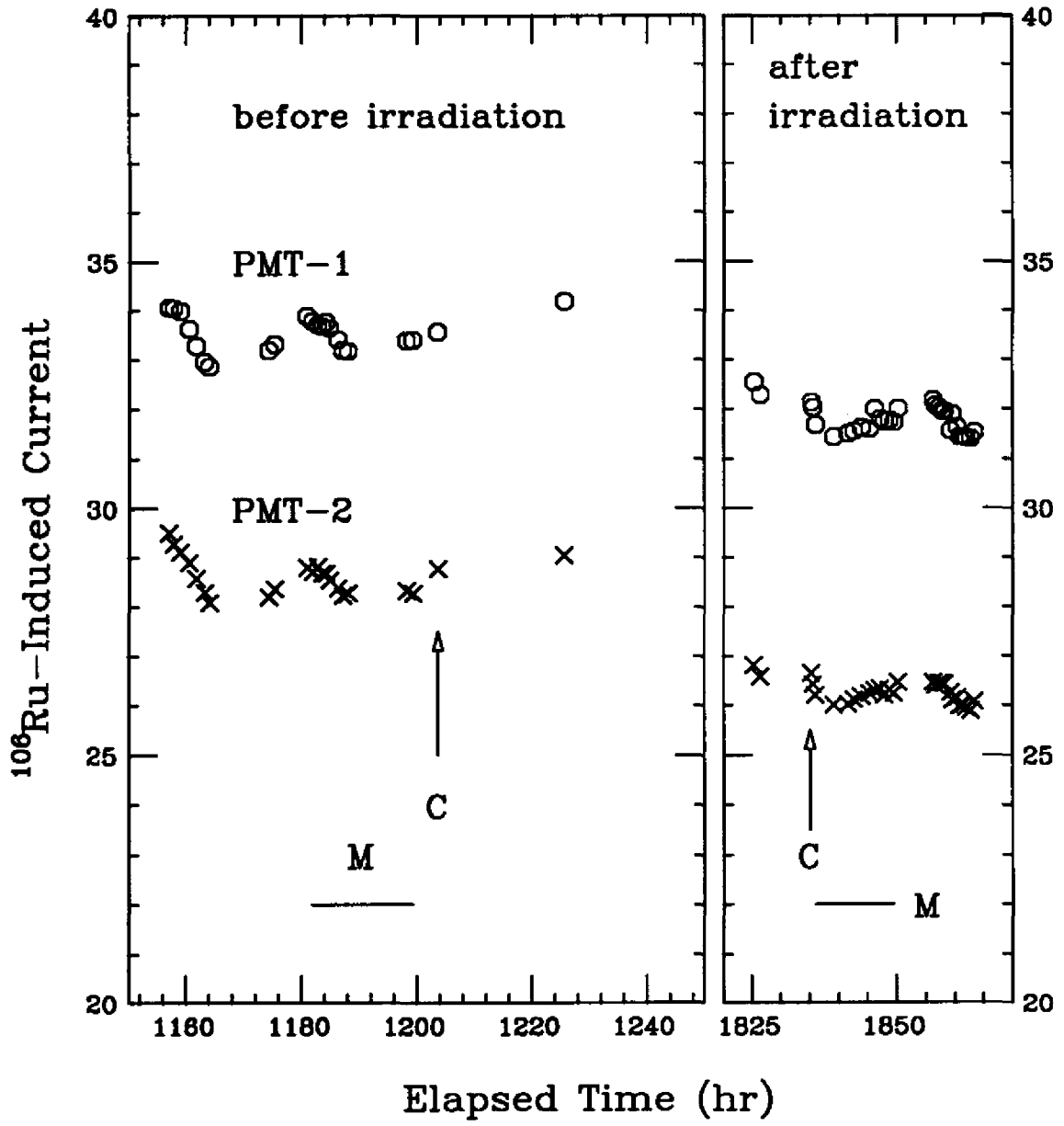

Figure 9: Gain stability of the PMTs for Module B. During the periods indicated by C and M, we performed (C) the pulse height and resolution calibration, and (M) the response mapping.

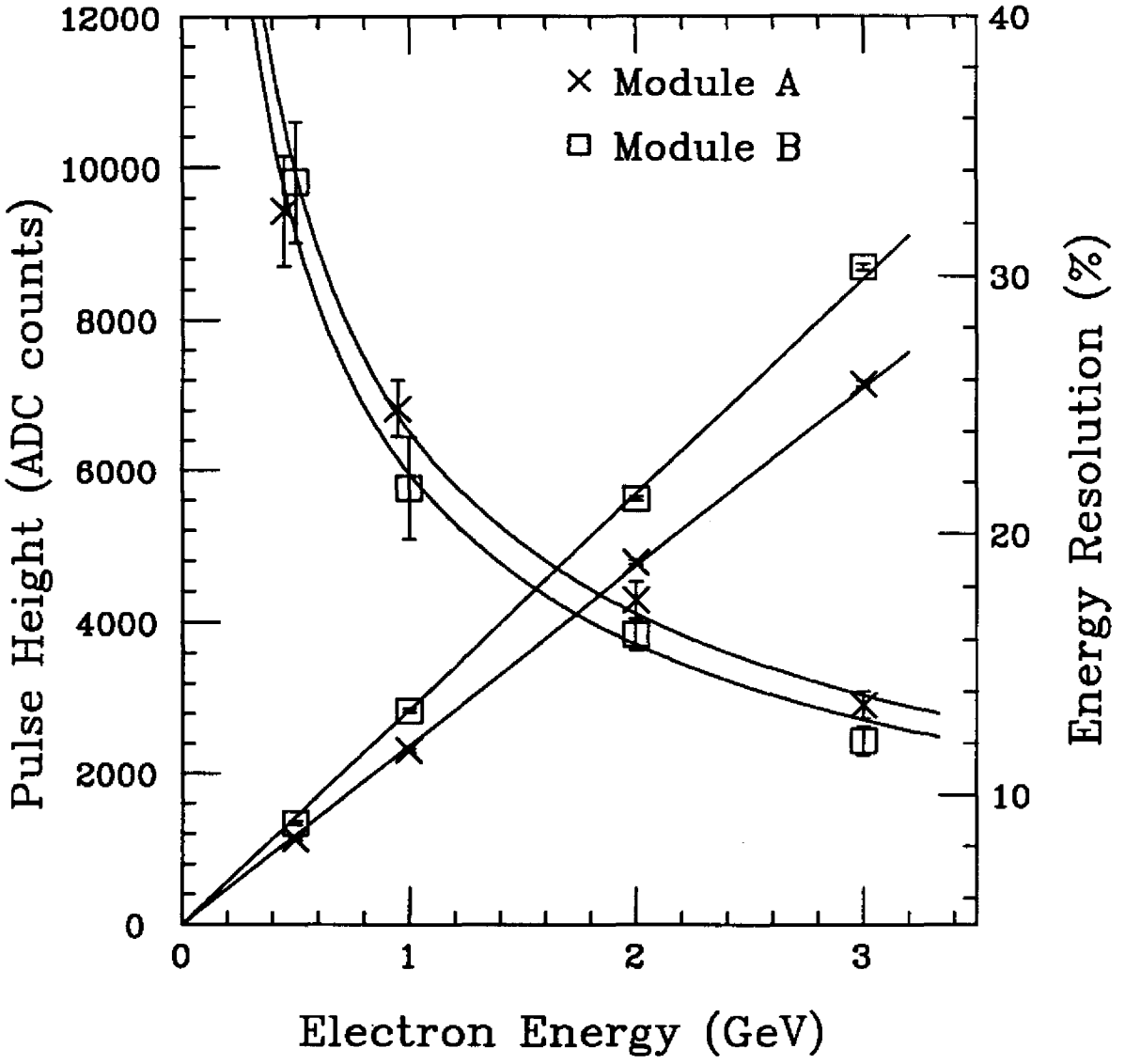

Figure 10: The measured energy responses and resolutions of Modules A and B. These data are after the irradiation. The energy resolutions are fitted well by $24\%/\sqrt{E}$ for Module A and $22\%/\sqrt{E}$ for Module B.

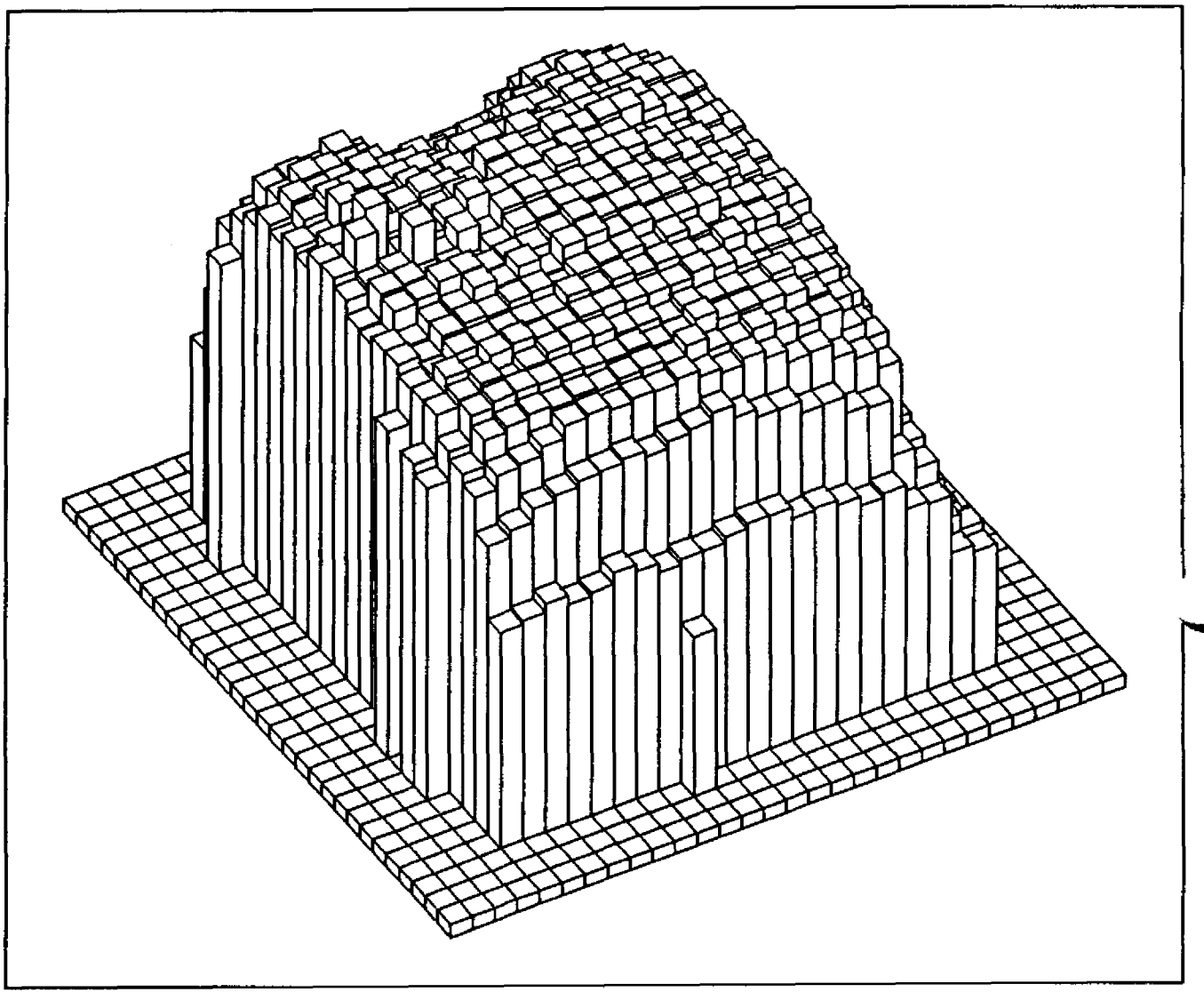

Figure 11: Lego plot of the response map of Module A after irradiation. The mesh size is 5 mm×5 mm.

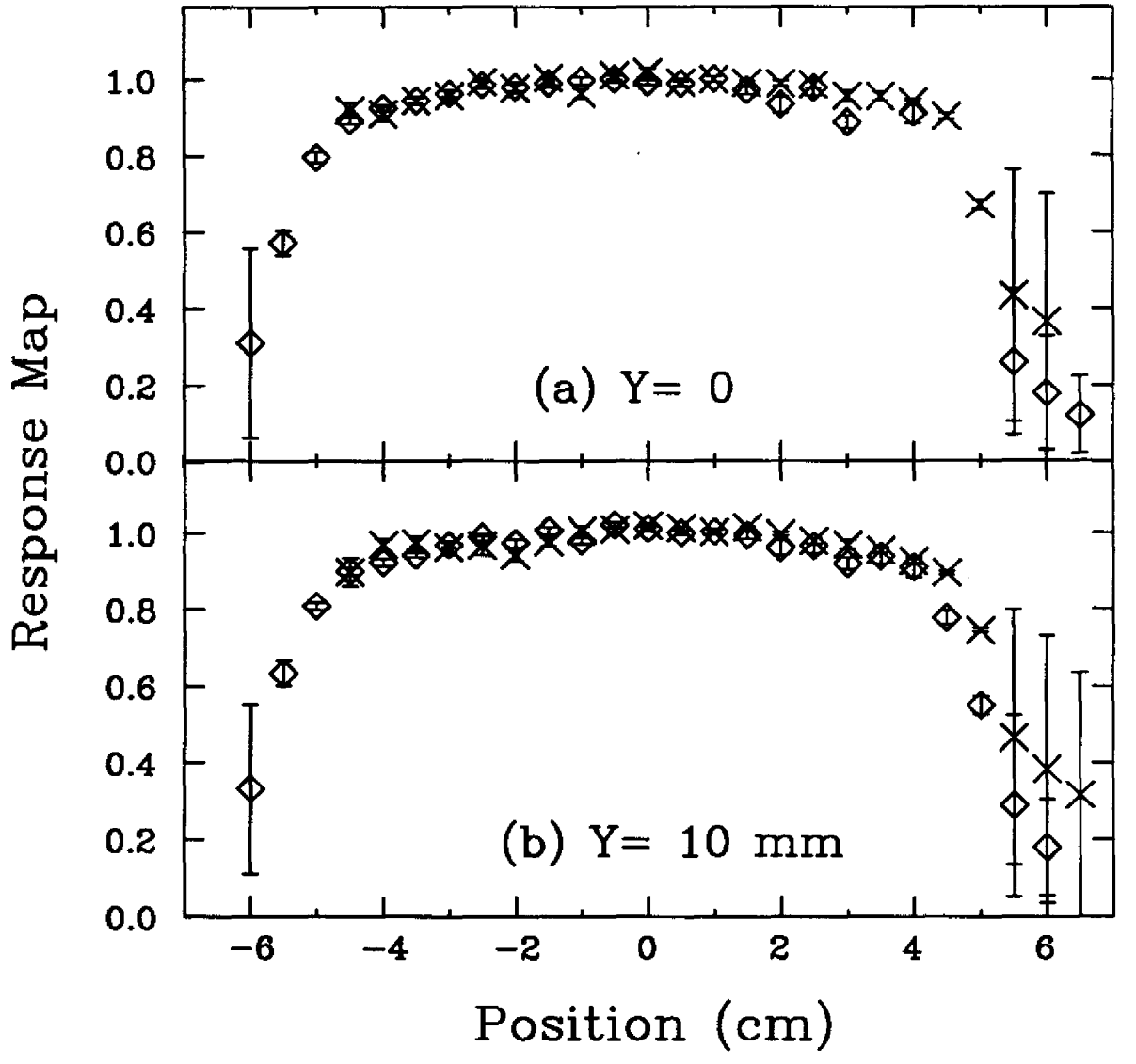

Figure 12: Response to 2-GeV electrons across the tile: (a) along the median line, (b) at 10 mm from the median line. The data are compared before (diamonds) and after (crosses) irradiation. The data are normalized at the center.

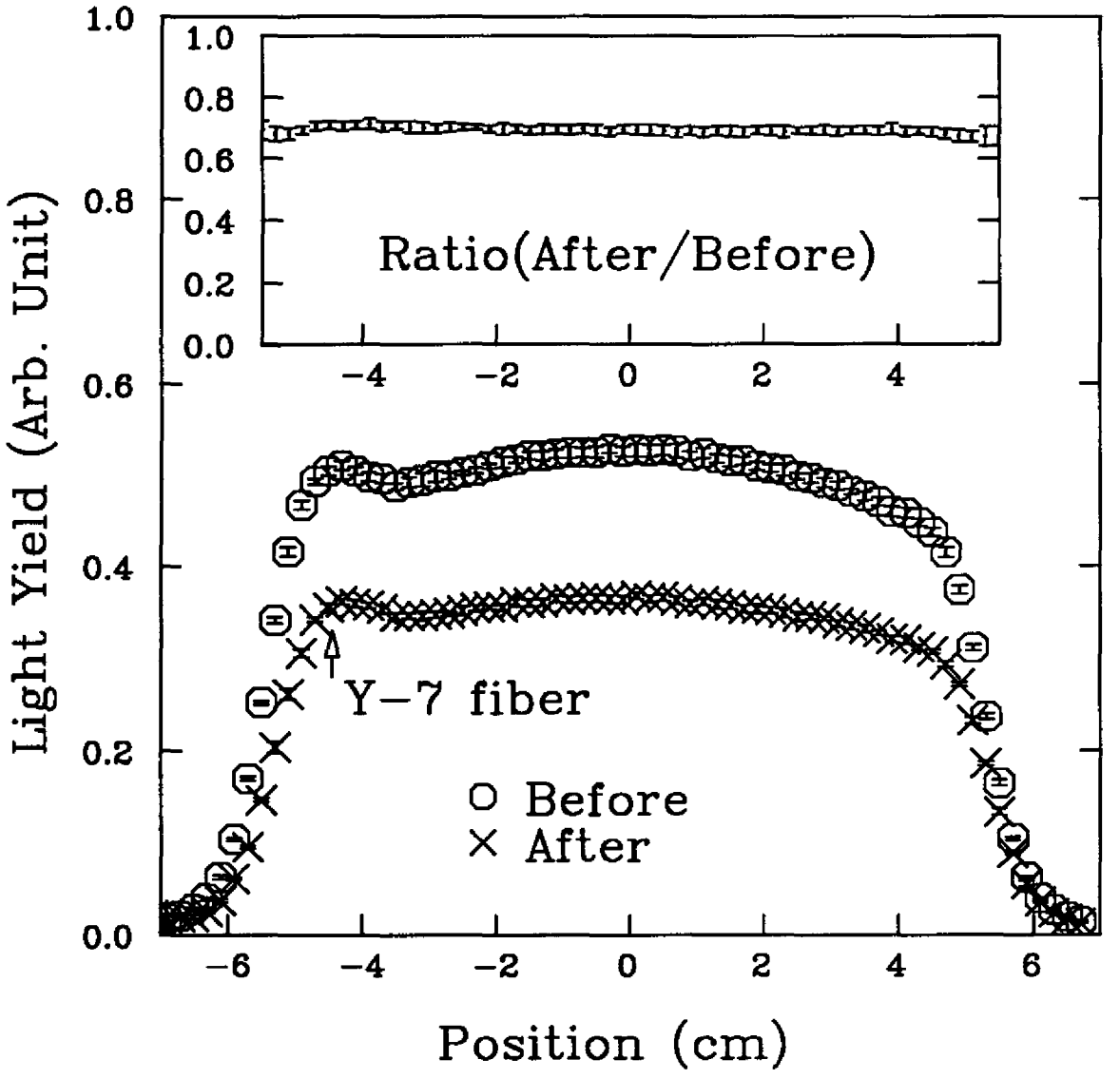

Figure 13: Response map of a tile/fiber assembly measured by scanning with a ^{106}Ru source. This assembly was non-uniformly exposed to ^{60}Co with a dose distribution of 0.62 Mrad at the center and 0.20 Mrad at the edge.

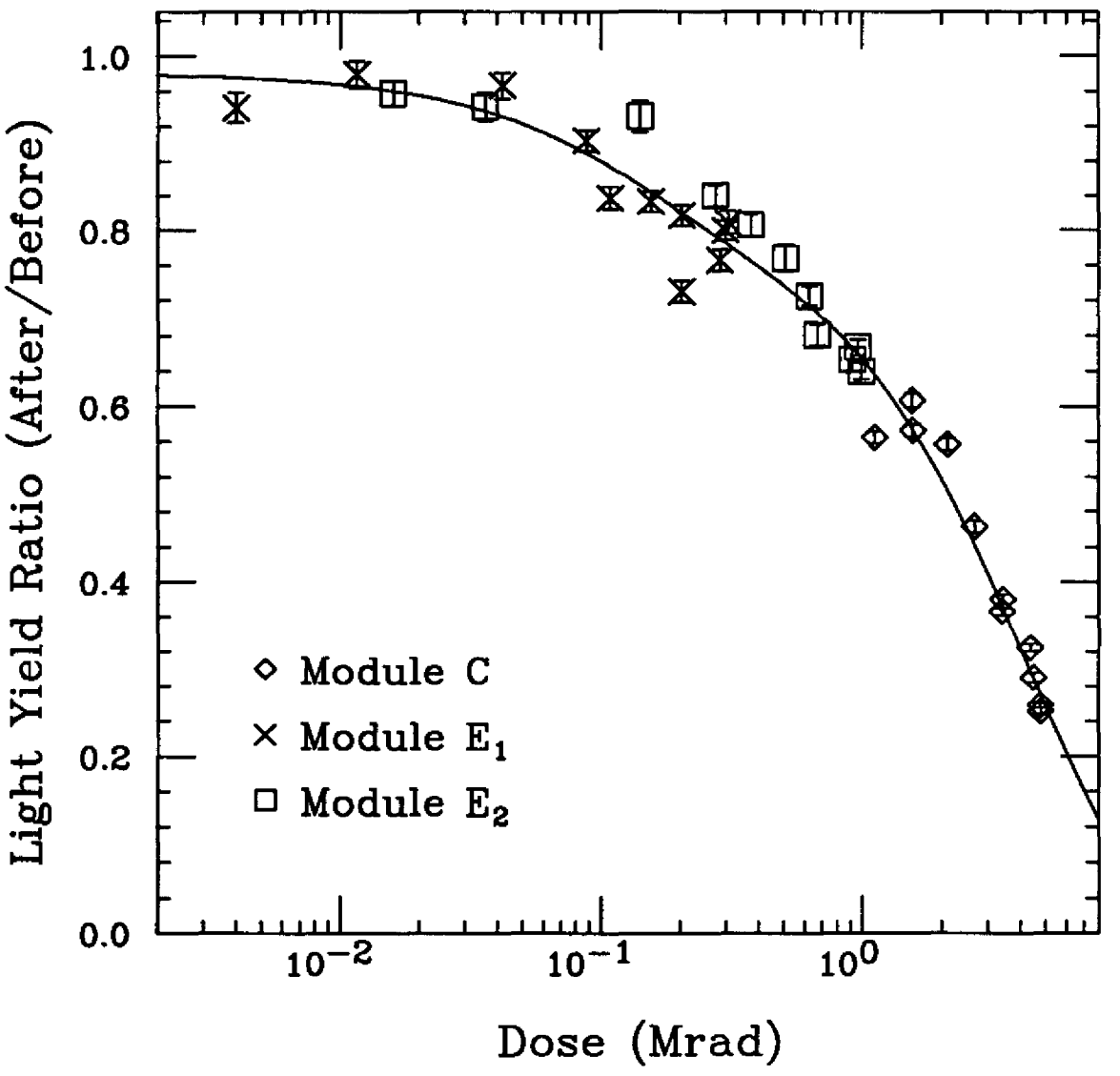

Figure 14: The 2.5-GeV electron shower induced damage as a function of the mean dose, measured with a ^{106}Ru source. The curve is a fit given by Eq. (1).

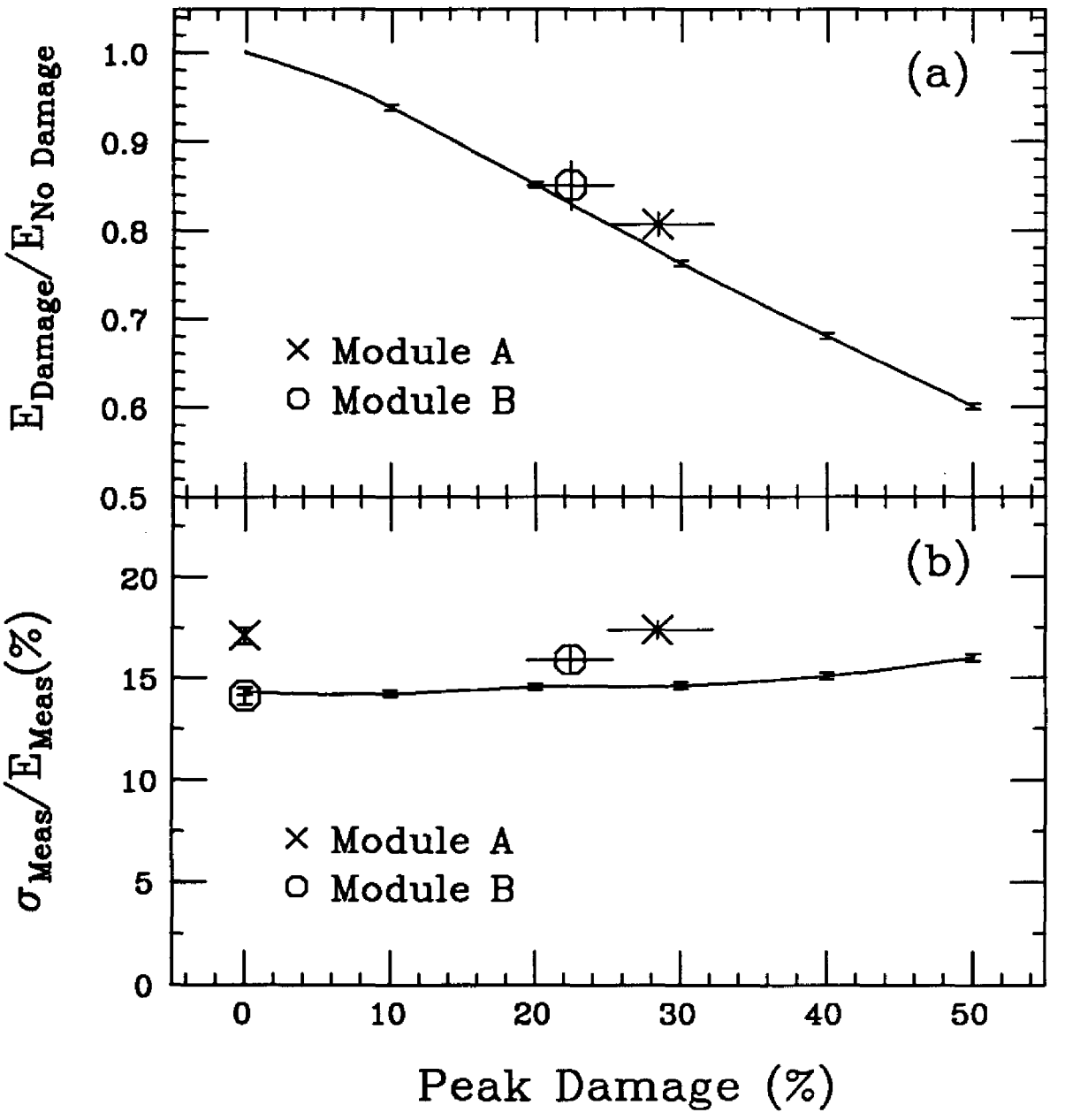

Figure 15: (a) Reduction of the energy response and (b) the energy resolution as a function of the peak damage. The solid lines are the simulation for 2-GeV electrons. The measured values for Modules A and B are shown by crosses and circles.

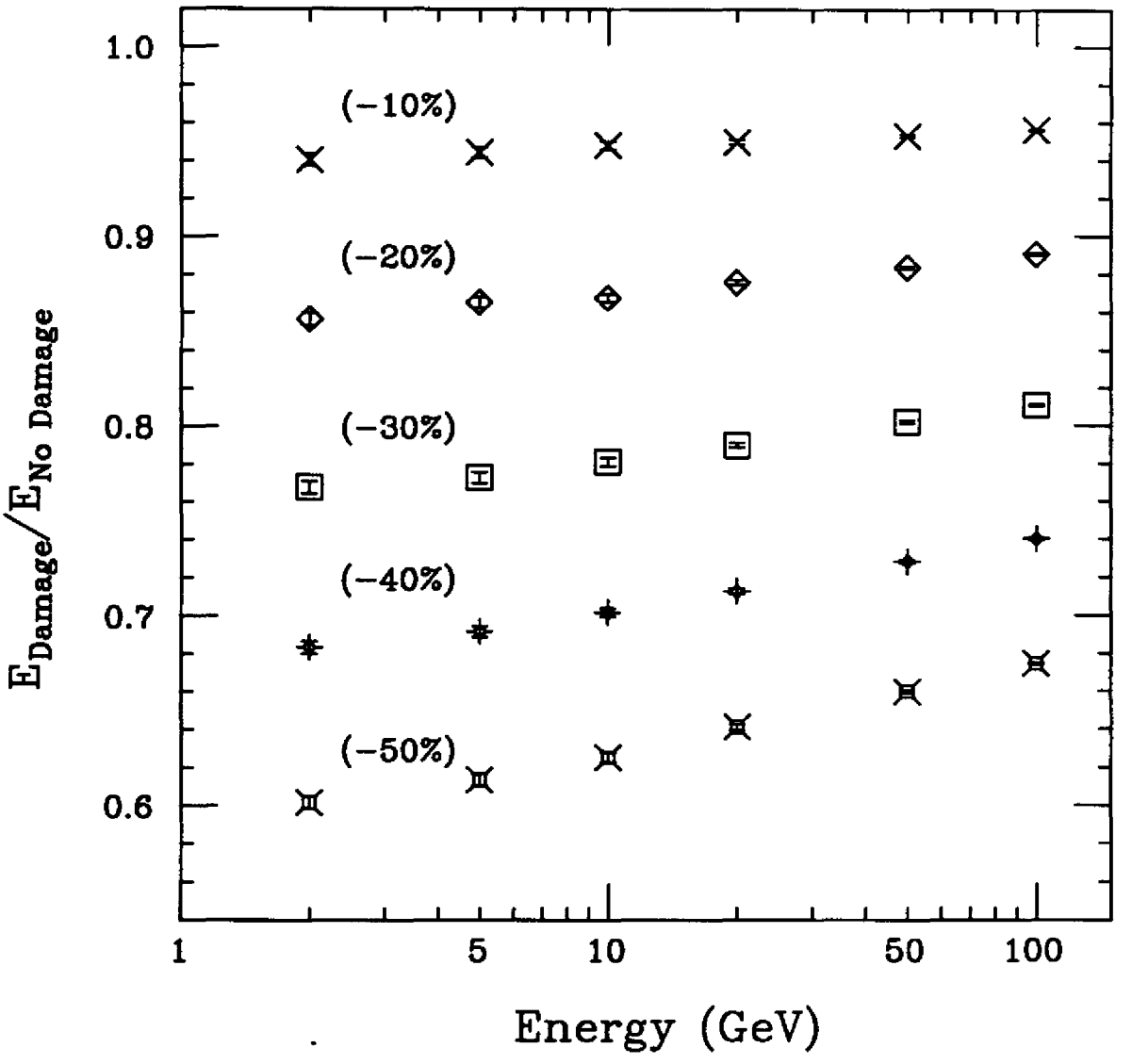

Figure 16: Reduction of the energy response as a function of the electron energy simulated for peak damages of 10% to 50%.

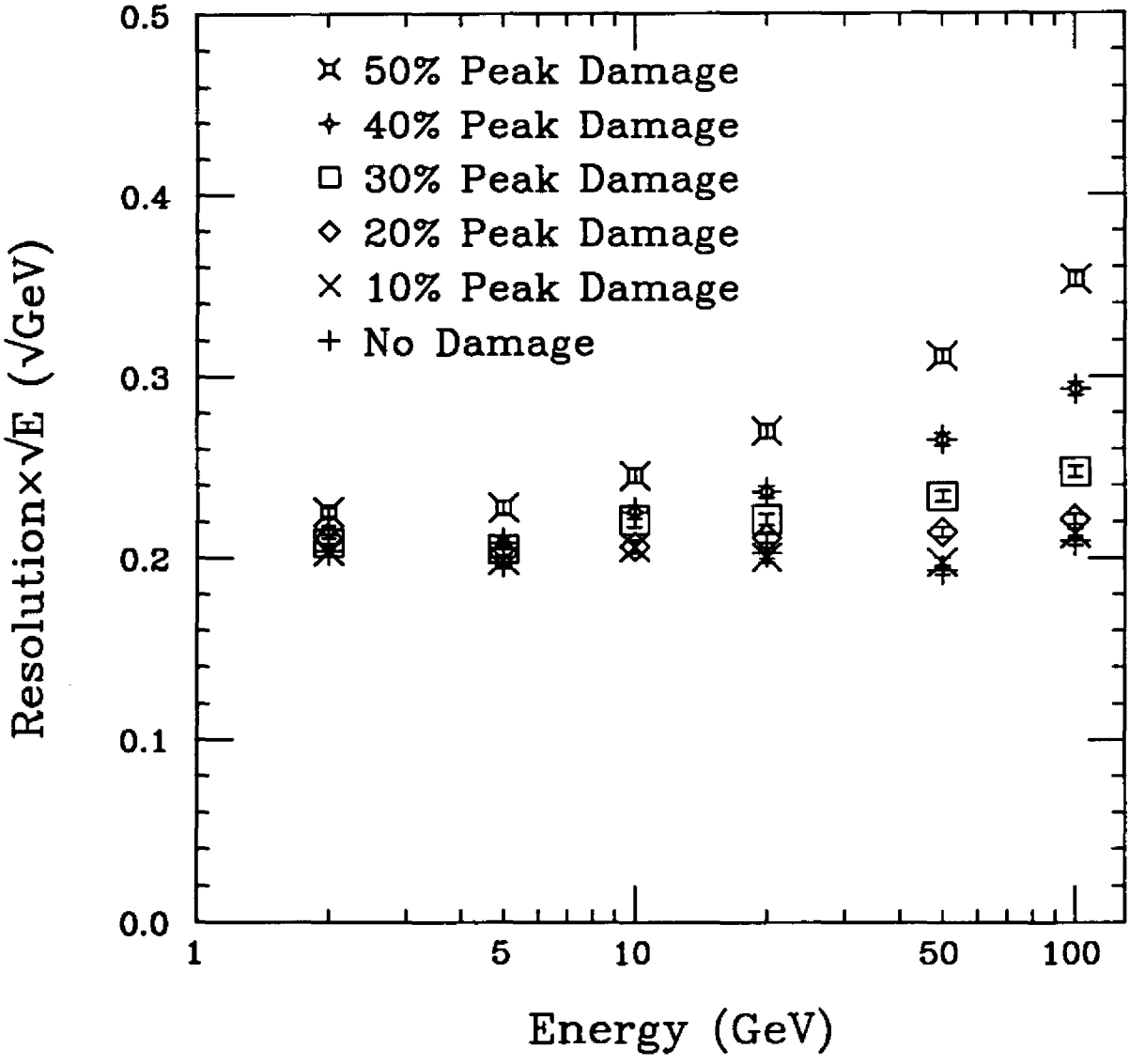

Figure 17: Resolution times $\sqrt{E}$ as a function of the energy. The simulation data are plotted for various peak damages up to 50%.

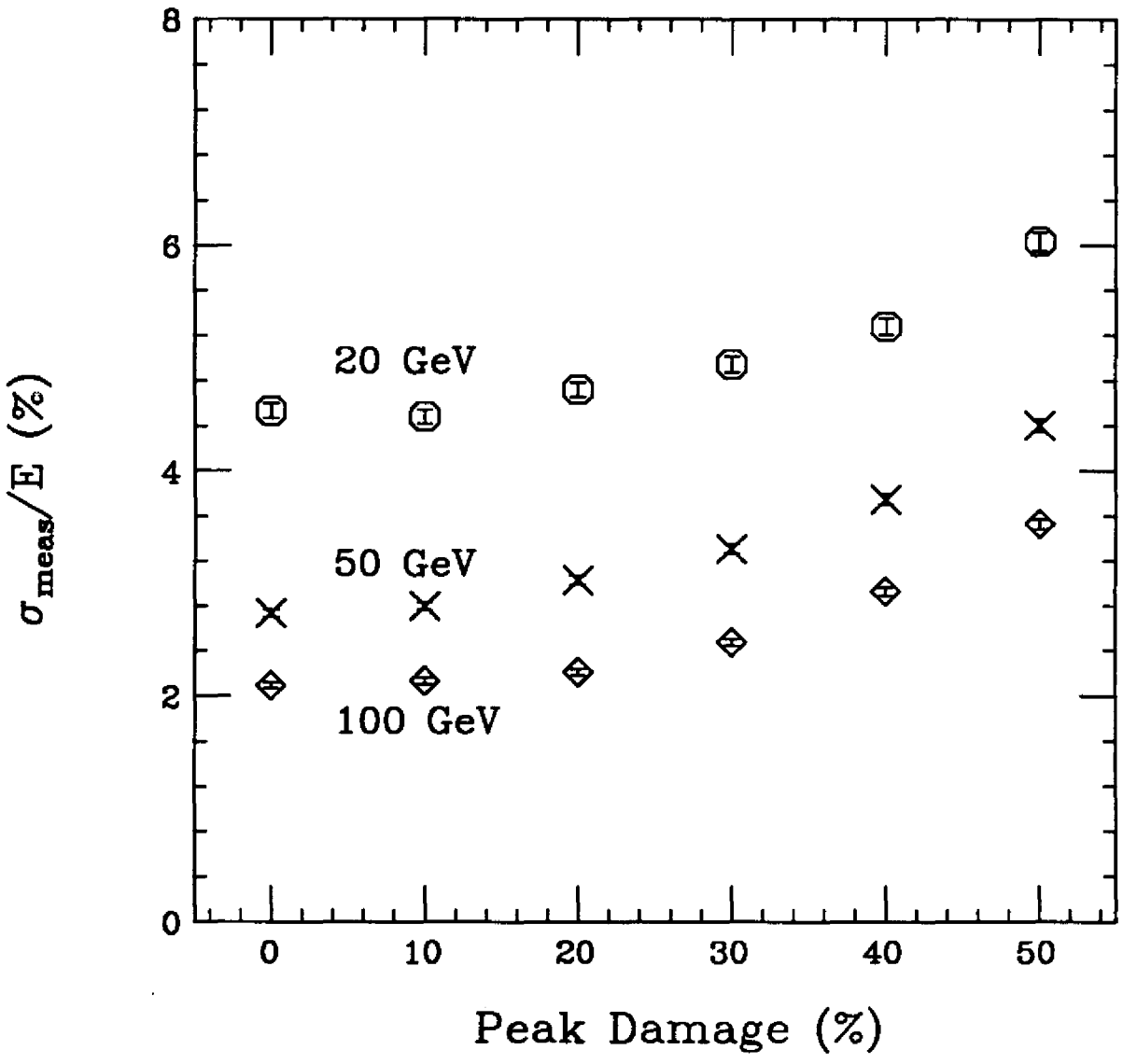

Figure 18: Resolution as a function of the peak damage for energies of 20, 50 and 100 GeV.

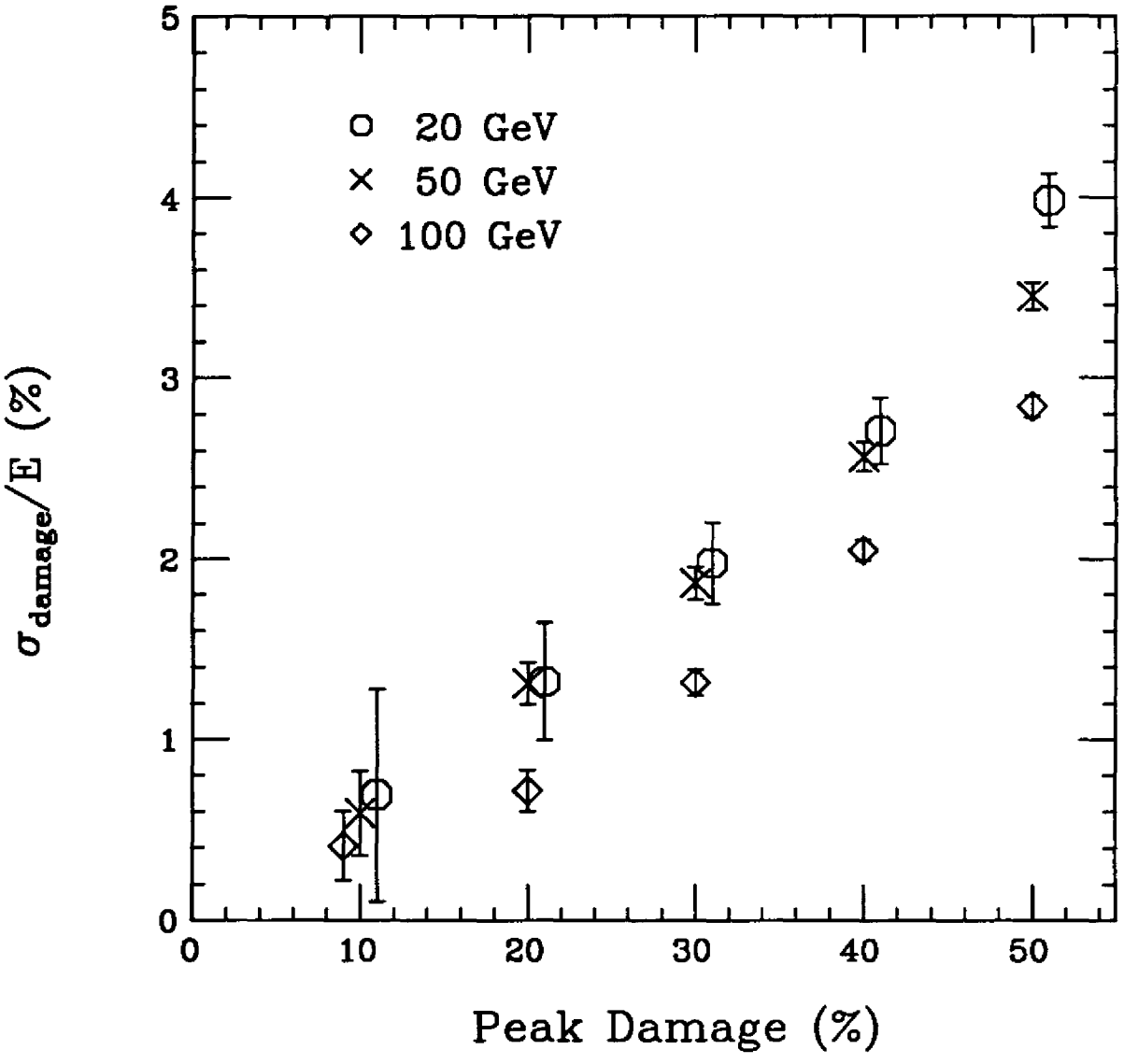

Figure 19: Damage-induced error to resolution as a function of the peak damage for energies of 20, 50 and 100 GeV.